



Cite this: DOI: 10.1039/d5fb00629e

Inducing covalent cross-links in soy protein films through ferulic acid incorporation and UV irradiation and its effect on film properties

Md Shakil, ^{ab} Tanjina Akter, ^a Nonthacha Thanathornvarakul ^a
and Thanachan Mahawanich ^{*a}

This study aimed to investigate the impact of ferulic acid (FA) and UV-C curing on the properties of soy protein isolate (SPI) films. The films were fabricated from SPI with 1.5% FA and subjected to UV-C radiation at three doses (1.56, 4, and 12 J cm⁻²) applied either to pre-formed films or film-forming solutions. The SPI film without FA and UV-C treatments was considered as a control. The mechanical, physicochemical, and morphological properties of the films were investigated. Protein cross-linking via C–N and dityrosine bonds was confirmed using FTIR and fluorescence spectroscopic techniques, respectively. FA addition significantly influenced thickness and transparency, but had little effect on tensile strength, elongation at break, film solubility, color values, water vapor permeability (WVP), and film hydrophobicity. Furthermore, UV-C treatment of either the film-forming solution or preformed FA + SPI films significantly improved tensile strength, elongation at break, hydrophobicity, and yellowness, while decreasing transparency compared to the control film. Exposure to UV-C at 12 J cm⁻², whether pre-formed films or film-forming solutions, increased tensile strength and elongation at break approximately 1.3 times and 1.7 times, respectively, compared to the control. UV-C exposure slightly increased WVP and had a minimal effect on film solubility compared to the control. The surface hydrophobicity of the films increased with higher doses, particularly in treatments applied to preformed films. The SEM micrographs revealed cracks and pinholes in the UV-treated film matrices. Our findings demonstrate that UV-C irradiation can effectively improve the tensile properties of SPI films containing ferulic acid.

Received 28th September 2025
Accepted 25th March 2026

DOI: 10.1039/d5fb00629e

rsc.li/susfoodtech

Sustainability spotlight

This research addresses the growing demand for eco-friendly and biodegradable packaging by investigating techniques to improve soy protein isolate (SPI) films with ferulic acid (FA) fortification and UV-C curing. Conventional plastic packaging significantly contributes to municipal solid waste, emphasizing the need for sustainable alternatives. The work promotes the application of SPI films, enhancing their mechanical and hydrophobic qualities, thus providing a potential way to lessen environmental impact. This supports UN Sustainable Development Goal 12 (Responsible Consumption and Production) by promoting the use of sustainable materials and methods. Additionally, it advances Goal 13 (Climate Action) by decreasing reliance on petroleum-based plastics. The study outlines a promising approach for advancing plant-based packaging toward a more sustainable future.

1 Introduction

Packaging may be considered an integral part of a food product, playing a role in protecting and maintaining the quality of the product inside. Petroleum-based packaging materials are popular due to their superior properties and lower cost. However, they may contribute to “white pollution” in the environment due to their non-biodegradable nature.¹ Annually, 376 million tons of plastic are produced and consumed globally,

with the majority remaining unchanged after their intended uses, causing serious environmental problems. Some plastics may break down into microplastics, which can infiltrate soil and water, raising concerns as they pose significant health risks when entering the food chain.^{2,3} With increasing environmental awareness and sustainability initiatives, researchers and the food industry are encouraged to reduce reliance on unsustainable packaging and explore alternative materials to conserve limited resources. This effort supports the global push toward sustainable food production and packaging, focusing on minimizing environmental impact, improving resource efficiency, and ensuring food safety. It emphasizes the importance of developing and adopting biodegradable packaging as an alternative to conventional plastics.^{4,5} Researchers have investigated

^aDepartment of Food Technology, Faculty of Science, Chulalongkorn University, Bangkok 10330, Thailand. E-mail: thanachan.m@chula.ac.th

^bDepartment of Dairy and Food Science, South Dakota State University, Brookings, South Dakota 57007, USA



renewable biopolymers, including polysaccharides, proteins, and lipids, as alternatives to non-biodegradable plastics due to their potential as a base for biodegradable packaging.⁶

Biodegradable packaging, made from renewable resources, is growing in popularity as a sustainable alternative that helps reduce waste and conserve resources. Proteins, among all biopolymers, exhibit superior mechanical properties as well as barrier properties against nonpolar compounds, such as oil and oxygen.⁷ The difference in the properties of amino acid side groups also renders proteins capable of being modified using various techniques. Researchers have developed packaging films using a range of food proteins such as soy, whey, peanut, gelatin, wheat gluten, sesame, and zein, due to their notable advantages. Among them, soy protein isolate, a byproduct of the soybean oil industry, contains more than 90% protein, which makes it an incredible, upcycled, renewable, and sustainable source for packaging materials. These sustainable materials can support circular economies by upcycling agricultural byproducts and encouraging environmentally responsible practices in food packaging. Soy protein has been extensively investigated for use in packaging films due to its excellent film-forming properties, eco-friendly nature, availability, and low cost.⁸ These soy protein films are transparent, flexible, and smooth, with excellent resistance to oil, oxygen, and organic volatiles.⁹ However, the inherent hydrophilic nature of the protein is responsible for the film's inferior mechanical and moisture barrier properties, making it less competitive than those made of petroleum-based polymers.¹⁰ Therefore, further research is needed to overcome these limitations and enhance the functional properties by modifying the reactive side groups of proteins through various protein cross-link-promoting treatments.¹¹

Different classes of chemicals, including aldehydes, phenolic compounds, and polycarboxylic acids, have been utilized as cross-linking agents in protein systems. Ferulic acid (FA), a natural and non-toxic phenolic compound found in plants, is recognized as generally recognized as safe (GRAS).¹² It exemplifies green chemistry techniques, such as cross-linking, which improve the sustainability of food packaging materials. According to Strauss & Gibson,¹³ the protein cross-linking mechanism begins with the oxidation of FA, with the production of its corresponding quinone. The quinone could react with the amino or sulfhydryl group of the polypeptide, forming a covalent C–N or C–S bond, and regenerating hydroquinone. This hydroquinone, again, can undergo oxidation and react with the amino or sulfhydryl group of another polypeptide chain, resulting in a covalent cross-link between two polypeptide chains. Alternatively, two polypeptides with quinone attached to each chain can dimerize to form a covalent cross-link. Cao *et al.*¹⁴ reported that ferulic acid was efficient in terms of improving the tensile strength of gelatin films owing to its protein cross-linking ability.

Applying UV-C radiation to enhance the functional properties of protein films illustrates how energy-efficient and non-toxic techniques can contribute to sustainable food packaging solutions. In UV irradiation, the conjugated double bond system of the aromatic ring of the side group of certain amino

acids, such as phenylalanine, tryptophan, and tyrosine, absorbs the radiation and undergoes free radical formation. Upon free radical recombination, a covalent cross-link is induced.¹⁵ UV-induced property modification has been investigated in various protein films.^{16–24} Gennadios *et al.*¹⁹ observed that, upon UV-C exposure, the soy protein film exhibited an increase in tensile strength accompanied by a decrease in elongation at break. However, the effect of UV radiation on protein film properties is inconsistent among various studies, likely because, in addition to promoting protein cross-linking, the radiation can also induce molecular degradation.^{25–27} Cho *et al.*²⁸ proposed that several factors, including protein concentration, oxygen availability, and the quaternary structure of the protein, influence the effect of irradiation on protein structure.

To the best of our knowledge, although several studies have investigated the effects of various combined treatments on different protein films, no research has specifically examined the combined effect of ferulic acid fortification and UV-C irradiation on soy protein films. Therefore, the objective of this study was to assess the combined effects of ferulic acid and UV-C treatment on the mechanical (tensile strength and elongation at break), optical (color and transparency), barrier (water solubility, water contact angle and water vapor permeability), morphological, and structural and chemical properties of soy protein films for sustainable solutions in the food packaging industry.

2 Materials and methods

2.1 Materials

Food-grade soy protein isolate (SPI) (90.20% protein, wet basis) and glycerol were purchased from Krungthepchemi (Bangkok, Thailand). Ferulic acid was obtained from Chanjao Longevity (Bangkok, Thailand).

2.2 Film preparation

Soy protein films were prepared according to the method described by Insaward *et al.*²⁹ with some modifications. 5 g of SPI and 2.75 g of glycerol were dissolved in 92.25 g of phosphate buffer (0.05 M, pH 7.4). The mixture was then homogenized for 2 min at 22 000 rpm. After that, the solution was heated to 70 °C for 30 min to partially denature the protein and then cooled to ambient temperature (25 °C). The film-forming solution was later sonicated to remove air bubbles. An aliquot (45 mL) of film-forming solution was cast onto a 150 mm × 150 mm PTFE-lined mold and dried at 40 °C for 24 h in a hot air oven (Mode PRI/30, Genlab Prime, Genlab Ltd., UK). Finally, the film was removed from the mold and stored at 50% relative humidity for 72 h before further analyses. The film was denoted as a SPI film and used as a control in this study.

2.3 Ferulic acid and UV-C treatments of soy protein films

For ferulic-modified films, ferulic acid concentration was fixed at 1.5% by weight of soy protein isolate. The film samples were prepared using a protocol similar to the control, except that



Table 1 Film samples with the corresponding ferulic acid addition and UV-C doses

Film samples	Ferulic acid addition (% by weight of SPI)*	UV-C doses (J cm ⁻²)	Exposure time (min)
SPI (control)	—	—	—
FA + SPI	1.5	—	—
FA + PFUV1.56	1.5	1.56	10
FA + PFUV4	1.5	4.00	27
FA + PFUV12	1.5	12.00	80
FA + FSUV1.56	1.5	1.56	10
FA + FSUV4	1.5	4.00	27
FA + FSUV12	1.5	12.00	80

after heating and cooling the film-forming solution to ambient temperature, 0.075 g of ferulic acid was added, and the solution was then homogenized for 2 min at 22 000 rpm. Subsequently, the film was cast, dried, and conditioned using the same method as the control film. This ferulic-added soy protein film was abbreviated as FA + SPI.

For UV treatment, UV-C radiation at a wavelength of 253.7 nm was applied to either the ferulic-added film-forming solution before the drying step (FA + FSUVxx, with xx denoting the UV-C dose in J cm⁻²) or the ferulic-added preformed film (FA + PFUVxx, with xx denoting the UV-C dose in J cm⁻²). The UV-C radiation was varied at three different doses (1.56, 4.00, and 12.00 J cm⁻²). Irradiation was performed in a UV-C cabinet (model PIS-88C, P Inter Supply, Bangkok, Thailand) with a radiation intensity of 2500 μW cm⁻². The exposure time was calculated using eqn (1) as follows.

$$\text{UV dose (J cm}^{-2}\text{)} = \text{UV intensity} \times \text{exposure time} \quad (1)$$

Where UV-C intensity was in μW cm⁻² and exposure time was in seconds.

All film samples were equilibrated at 50% RH and 25 °C for 72 h before further analysis. The film samples used in this study are summarized in Table 1.

2.4 Fourier transform infrared (FTIR) spectroscopy

The formation of the C–N bond was monitored using an FTIR spectrometer (model Spectrum One, PerkinElmer, Waltham, MA, USA) with an attenuated total reflectance (ATR) accessory. Transmittance in a wavenumber range of 4000–500 cm⁻¹ was measured using a scanning resolution of 4.00 cm⁻¹ and 64 scans per sample.

2.5 Fluorescence spectroscopy

Dityrosine cross-linking was monitored using a spectrofluorometer (model FP-6200, Jasco, Tokyo, Japan) with an excitation wavelength of 320 nm. Emitted fluorescence, characteristic of dityrosine, can be detected in the emission wavelength range of 340–500 nm.³⁰ The scanning speed of the spectrofluorometer was set at 125 nm min⁻¹.

2.6 Film thickness and mechanical properties

To assess mechanical properties, a 100 mm × 30 mm strip was cut from the film sample. The thickness was measured with a thickness gauge (model 7301, Mitutoyo, Tokyo, Japan) at ten different points along the strip. The average thickness was then calculated.

The tensile test on the film samples was conducted in accordance with the ASTM D882 standard method³¹ for uniaxial tension. The test was performed using a Texture Analyzer (model TA.XTplus, Stable Micro System, Godalming, UK) equipped with tensile grips (A/TG probe). First, the machine was calibrated according to the manual, and then a film strip was clamped between the grips (initially set 50 mm apart). The film was then stretched at a constant speed of 8.33 mm s⁻¹ until it ruptured. Tensile strength (TS) and elongation at break (EB) were determined using eqn (2) and (3), respectively.

$$\text{Tensile strength (MPa)} = F/w.d \quad (2)$$

where F is the maximum force applied before failure (N), w is the initial film width (mm), and d is the initial film thickness (mm).

$$\text{Elongation at break (\%)} = \frac{L_f - L_i}{L_i} \times 100 \quad (3)$$

where L_f = final length of the film at break (mm) and L_i = initial gauge length of the film before testing (mm).

2.7 Water vapor permeability

The water-vapor permeability of the film samples was determined according to the ASTM E96-95 method.³² A film sample, free of leaks and scratches, was cut into a 60 mm × 60 mm piece. 20 g of dried silica gel was placed into a glass permeation cup. Silicone grease was applied to the rim of the cup. After being mounted on the cup, the film piece was tightened with a rubber ring and parafilm. The cup was weighed, placed in a distilled water chamber, and equilibrated at 25 °C. The weight of the permeation cup was taken every 24 h for seven days and calculated for the water vapor permeability using eqn (4):

$$\text{Water vapor permeability} = \frac{Wd}{At(P_2 - P_1)} \quad (4)$$

where W is the weight gain of the permeation cup (g); d is the film thickness (m); A is the exposed area of the film available for water permeation; t is the time to reach equilibrium (h); and $(P_2 - P_1)$ is the difference in partial pressure of water vapor across both sides of the film (Pa).

2.8 Water solubility

The water solubility of the film samples, expressed in terms of total soluble matter, was determined according to the method outlined by Insaward *et al.*³³ A 20 mm × 20 mm piece of film sample and Whatman grade 4 filter paper were dried in a hot air oven (Mode PRI/30, Genlab Prime, Genlab Ltd., UK) at 70 °C for 24 h. The initial dry weight of the dried film and filter paper was recorded. The film sample was then placed into a 50-mL test



tube containing 20 mL of distilled water, and the tube was continuously shaken using an Innova® laboratory shaker (model 2050, New Brunswick Scientific, Edison, NJ, USA) at room temperature (25 °C) for 24 h. Subsequently, the sample was filtered through the dried filter paper. The filter paper and the retained material were dried at 70 °C for 24 h and then weighed to determine the final dry weight. The water solubility was calculated using eqn (5)

$$\text{Water solubility (\%)} = \frac{W_i - W_f}{W_i} \times 100 \quad (5)$$

where W_i is the initial dry weight of the film sample (g), and W_f is the final dry weight of the film sample (g).

2.9 Surface hydrophobicity

The surface hydrophobicity of the films was evaluated by measuring the contact angle between a water droplet and the film surface using a contact angle measuring instrument (model OCA15EC, Data Physics Instruments, Filderstadt, Germany). A 4 μL drop of distilled water was placed on the film surface, and the contact angle (θ) formed between the droplet and the surface was recorded. Hydrophilic surfaces are indicated by contact angles less than 90° ($\theta < 90^\circ$), whereas hydrophobic surfaces show angles greater than 90° ($\theta > 90^\circ$).

2.10 Film density

Film density was calculated from dry mass and dimensions of a film piece as outlined by Fathi *et al.*¹⁶ using eqn (6):

$$\text{Film density} = \frac{m}{Ad} \quad (6)$$

where m is the dry mass of the film piece (g), A is the film area (cm^2), and d is the film thickness (cm).

2.11 Transparency

The transparency of a film sample was evaluated based on the % transmittance. First, a film sample was precisely cut to 10 mm by 40 mm. Then, the sample was mounted inside a glass cuvette. %Transmittance was measured at 500 nm using a visible spectrophotometer (model GENESYS20, Thermo Scientific, Waltham, MA, USA).

2.12 Film color

A chromameter (model CR400, Konica Minolta Sensing, Osaka, Japan) was used to determine the film color in the CIELAB system with a 10° observer and D65 illuminant. Measurements were taken at ten random places on each film sample and averaged to represent the color values of each replicate. Hue angle and chroma were also calculated from the CIE L^* , a^* , b^* using eqn (7) and (8):

$$\text{Hue angle (Quadrant II)} = 180 + \arctan(b^*/a^*) \quad (7)$$

$$\text{Chroma} = (a^{*2} + b^{*2})^{1/2} \quad (8)$$

2.13 Film microstructure

The cross-sectional microstructure of films was examined using a scanning electron microscope (model JSM-IT300, JEOL, Tokyo, Japan). The film sample was initially cut into a five mm-wide strip and stored in a desiccator with silica gel for seven days to ensure thorough drying. Following this, the film sample was carefully sectioned using a sharp razor blade to reveal a clean cross-sectional area. The prepared sample was then mounted on a sample stub and coated with a layer of gold using a sputter coater. Finally, the microstructure of the film matrix was observed at 800 \times magnification.

2.14 Statistical analysis

All experiments were conducted in triplicate, and a completely randomized design CRD was used. One-way analysis of variance (ANOVA) was performed on all experimental data using SPSS (IBM SPSS Statistics 22) software. Duncan's multiple-range test was used to assess differences among sample means at the 0.05 significance level.

3 Results and discussion

3.1 FTIR analysis

The FTIR spectra of the SPI, FA + SPI, FA + PFUV12, and FA + FSUV12 films are shown in Fig. 1. FTIR analysis was carried out to monitor the development of the C–N bond induced by ferulic acid cross-linking of protein. All film samples exhibited a consistent pattern, with transmittance in the region 1000–1140 cm^{-1} experiencing a slight decrease as the incorporation of ferulic acid (FA) and UV-C treatment intensified. Ikhmal *et al.*³⁴ reported that a prominent absorption peak appeared at 1040 cm^{-1} , which corresponds to the C–N stretching vibration typically associated with the cross-linking of proteins through FA addition. The FA + SPI film exhibited a slight reduction in transmittance compared to the control, indicating some degree of protein cross-linking caused by the addition of FA. However, the greater reduction in transmittance occurred in the FA + PFUV12 and FA + FSUV12 films in the region around 1040 cm^{-1} . This reduction may be due to UV-C treatment, which promotes the oxidation of ferulic acid to its corresponding quinone. This form is more efficient in cross-linking proteins than the unoxidized form. Adilah *et al.*³⁵ reported that FA contributes to

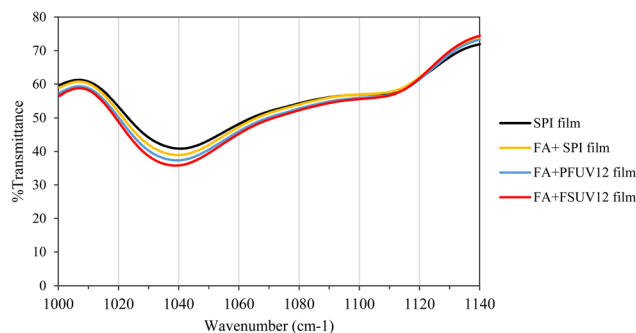


Fig. 1 FTIR spectra of treated and untreated soy protein isolate films.



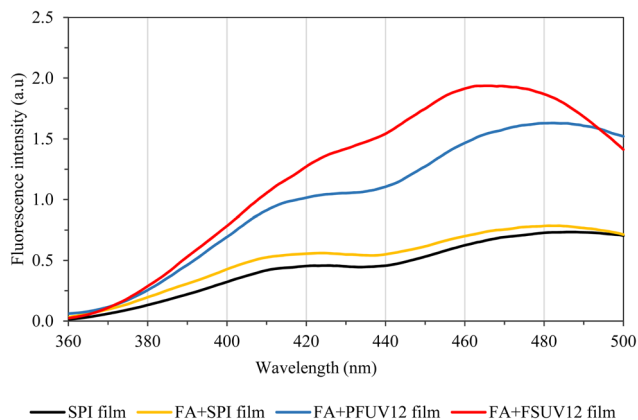


Fig. 2 Fluorescence emission spectra of treated and untreated soy protein isolate films.

protein cross-linking, which is further enhanced by oxidation. The FA + FSUV12 films exhibited a greater reduction in transmittance compared to the FA + PFUV12 films, likely due to the way UV-C irradiation was applied. When UV-C radiation is applied to the film-forming solution (FA + FSUV12), the protein matrix is more fluid, which allows the FA-quinone to disperse more evenly and cross-link the proteins more effectively. In the preformed film (FA + PFUV12), where the protein matrix is already established, it restricts the movement of the reactive FA-quinone species, thus decreasing cross-linking.^{16,36}

3.2. Fluorescence spectroscopy analysis

Dityrosine is formed in many proteins as a result of UV irradiation,^{37,38} and gamma-irradiation.³⁹ In these cases, dityrosine cross-linking can be either intra- or inter-molecular³⁸ and could result in protein aggregation.⁴⁰ Dityrosine is one of the specific markers of protein oxidation, especially for that induced by radiation. In this study, dityrosine cross-linking of the film samples was monitored using fluorescence spectroscopy. Al-Hilaly *et al.*³⁰ reported that dityrosine produces a specific fluorescence peak at 340–500 nm, with the highest intensity in the wavelength range of 400–420 nm. Correia *et al.*¹⁵ monitored dityrosine formation in insulin exposed to UV and detected the

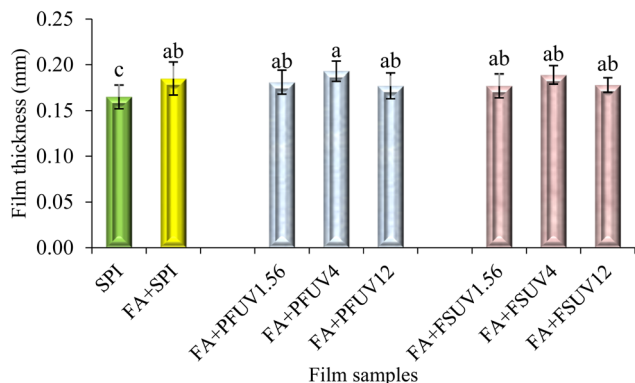


Fig. 3 Thickness of treated and untreated soy protein isolate films.

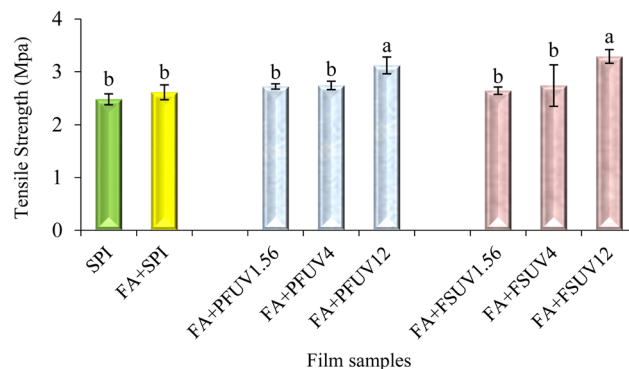


Fig. 4 Tensile strength of treated and untreated soy protein isolate films.

dityrosine peak in the wavelength range of 350–550 nm, with the greatest intensity around 405 nm. The fluorescence emission spectra of the film samples are shown in Fig. 2. This study detected a fluorescence peak confirming dityrosine formation in the wavelength range of 360–500 nm, with the highest intensity around the wavelength of 470 nm. It was evident that the UV-treated samples possessed greater fluorescence intensity than the unirradiated samples (SPI and FA + SPI films). Fluorescence intensity was found to increase with increasing UV-C dose. In this experiment, the FA + FSUV12 film exhibited higher fluorescence intensity than the FA + PFUV12 film.

3.3. Film thickness and mechanical properties

As shown in Fig. 3, the film thickness ranged from 0.165 to 0.193 mm. Adding FA or FA + UV-C treatment to SPI films significantly affected ($p \leq 0.05$) the film thickness, as the control film exhibits a lower thickness than the treated films. However, there were no statistically significant differences in thickness among all FA + UV-C treated films ($p > 0.05$). Nuthong *et al.*⁴¹ observed that adding up to 3% ferulic acid had no significant effect on the thickness of the porcine plasma protein-based film compared to the control. In another investigation, Díaz *et al.*¹⁸ examined the impact of UV irradiation on

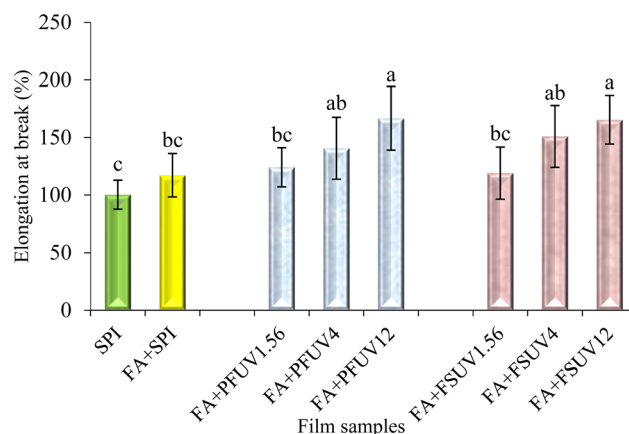


Fig. 5 Elongation at break of treated and untreated soy protein isolate films.



they protein concentrate films at various doses. They found that films treated with UV-C at doses of 0.12, 4.00, and 12.00 J cm⁻² exhibited increased thickness compared to the untreated film. The increase in thickness might be due to induced protein aggregation that may influence the structure of the film.¹⁸

Mechanical properties, including tensile strength (TS) and elongation at break (EAB) of the films, are summarised in Fig. 4 and 5, respectively. An increasing trend in tensile strength and elongation at break of SPI films was observed upon incorporation of FA and/or UV-C curing. However, most treatments did not result in statistically significant improvements in TS or EAB, except for the treatment at the highest UV-C dose (12 J cm⁻²) compared to the control. Insaward *et al.*³³ documented that incorporating either oxidized or unoxidized FA at a concentration of 1.5% into soy protein isolate films resulted in an enhancement in tensile strength and elongation at break of the film. In another study, Ou *et al.*⁴² also observed that incorporating FA at concentrations ranging from 50 to 200 mg/100 g into soy protein isolate films improved the tensile strength and elongation at break of the film. This improvement in tensile properties may be attributed to the development of a cross-linked structure resulting from reactions between protein and FA.³³ Conversely, Arcan and Yemencioğlu⁴³ reported an opposite finding, noting that the addition of ferulic acid led to a decrease in tensile strength but an increase in elongation at break in zein films. UV-C irradiation of either the FA-added preformed film (FA + PFUV) or film-forming solution (FA + FSUV) resulted in an upward trend in tensile strength as the UV-C dose increased.

The films (FA + PFUV12 and FA + FSUV12) subjected to the highest UV-C dose (12 J cm⁻²) showed the most significant increase in tensile strength, likely due to enhanced protein cross-linking, as proven in Fig. 1 and 2. Both film samples demonstrated an approximately 1.3-fold increase in tensile strength compared to the control. However, at the same radiation level, UV-C treatment of preformed films and of the film-forming solution demonstrated statistically similar effects on tensile strength. Díaz *et al.*¹⁸ found that UV-C exposure of whey protein film-forming solutions was more effective at enhancing tensile strength than treating preformed films at the same dose level. Our study also follows the findings of Díaz *et al.*¹⁸ where the UV-C exposure of the film-forming solution (FA + FSUV12 film) resulted in greater TS. A higher reduction in the transmittance of ATR-FTIR spectra supports the improved TS of the FA + FSUV12 film, indicating a higher degree of cross-linking when a higher UV-C dose was applied to the film-forming solution. The same UV-C dose (12 J cm⁻²) applied to the preformed film resulted in lower TS, although this difference was not statistically significant compared with the FA + FSUV12 film ($p > 0.05$). This apparent discrepancy can be attributed to several factors. ATR-FTIR mainly probes the surface region (penetration depth $\approx 0.5\text{--}5\ \mu\text{m}$),^{44,45} whereas tensile testing reflects the bulk mechanical response. An enhancement in tensile strength was reported by Díaz *et al.*¹⁸ when the whey protein concentrate films were exposed to a high UV-C dose of 12.00 J cm⁻². Our study also aligns with the findings of Akter *et al.*,⁴⁶ who reported

that UV-C treatment at 12 J cm⁻² increased the tensile strength of soy protein isolate films.

For elongation at break, the addition of FA to SPI films and UV-C exposure of FA-added films were found to increase the elongation at break (EAB) of the films, as shown in Fig. 5. UV-C exposure at 4.00 and 12.00 J cm⁻², applied to the film-forming solution and the preformed FA + SPI film, significantly increased the EAB compared to the control film. The FA + FSUV12 and FA + PFUV12 films showed approximately 1.7 times higher elongation at break. The improved mechanical properties of FA + SPI films upon exposure to high doses of UV-C could be due to the induced protein cross-linking, as proven in Fig. 1. Although the FA + FSUV12 film sample reveals the greatest reduction of ATR-FTIR spectra transmittance, the FA + FSUV12 and FA + PFUV12 films showed statistically similar results.

A higher crosslink density can enhance stiffness but reduce deformability, hinder the movement of SPI chains and limit energy absorption, resulting in a more brittle matrix and no further improvement in ultimate EB. Similar behavior was found in the Tara pod extract-soy protein isolate film⁴⁷ and a tannic acid-containing whey protein film.⁴⁸ Masutani *et al.*⁴⁹ stated that Aromatic amino acids, particularly tyrosine, can absorb UV radiation, leading to the formation of an acid-free radical (Tyr[•]). The recombination of these free radicals results in the formation of dityrosine cross-links, both inter- and intramolecularly. As observed in Fig. 2, emission peaks at around 470 nm, which are in a typical range of dityrosine, were noticeable for higher UV-C doses. In addition to dityrosine, isodityrosine and trityrosine may also be formed, although typically at lower concentrations compared to dityrosine.¹⁵ Rhim *et al.*²⁴ observed the formation of covalent bonds, aside from disulfide bonds, within the structure of UV-treated SPI films. Moreover, the formation of cross-linked structures in the UV-treated FA + SPI films enhances the film integrity, which could be a possible explanation for the increase in tensile strength along with elongation at break.

3.4. Film density

The density of SPI films seemed to be unaffected by FA addition and FA + UV-C treatment, as presented in Fig. 6. The density of

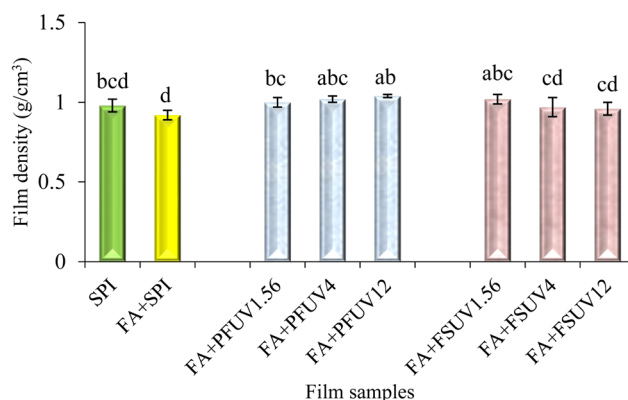


Fig. 6 Density of treated and untreated soy protein isolate films.



the films was approximately 1 g cm^{-3} . This finding is in contrast to the previous findings of Fathi *et al.*¹⁶ They found that sesame protein films exposed to UV-A, UV-B, and UV-C at a dosage of 32.6 J cm^{-2} significantly increased the density of the films. The dissimilarity observed in our findings may be attributed to the application of lower radiation doses compared to those employed by Fathi *et al.*¹⁶

3.5 Barrier properties

The water vapor permeability (WVP) of SPI and treated SPI films is depicted in Fig. 7. The WVP of the SPI films was unaffected by either FA addition or FA + UV-C treatments. Compared to the control, the addition of FA and FA + UV-C treatment to the films slightly increased WVP. However, all the film samples exposed to UV-C radiation exhibited statistically similar WVP, ranging from 5.40×10^{-7} to $6.43 \times 10^{-7} \text{ g m m}^{-2} \text{ h}^{-1} \text{ P}$. This uniformity indicates that the hydrophilic characteristics of the protein film may override the impact of increased cross-linking.⁵⁰ In addition, the SPI contains both polar and non-polar groups. Polar amino acid residues and peptide segments readily interact with water molecules through hydrogen bonding, facilitating moisture diffusion despite the formation of new covalent bonds. Moreover, the arrangement of protein molecules, microvoids, and the presence of plasticizers can further offset the expected barrier improvement.⁴⁸ Previous research on phenolic cross-linking in protein films has shown mixed results concerning its impact on WVP. González *et al.*⁵¹ suggested that phenolic compounds may interact with proteins *via* various interactions, such as hydrogen bonds and covalent bonds, resulting in a protein matrix with reduced free volume. Consequently, this alteration allows water vapor to permeate the film matrix at a slower rate. On the other hand, another study showed that although adding a certain level of ferulic acid (FA) improved mechanical properties, the WVP of SPI films did not decrease significantly and even increased at higher doses.⁴² Strauss & Gibson⁴³ reported that using a higher concentration of phenolic acid may cause the polymerization of phenolics rather than reacting and cross-linking with proteins. This may increase the WVP of the phenolic-added (FA) film. The minimal effect of phenolic addition on WVP was also reported by Insaward *et al.*³³ for soy protein films and Wang *et al.*⁵² for whey protein films.

In the case of UV-C curing, some studies also observed that UV-C exposure of whey protein films^{50,53} and soy protein films (Gennadios *et al.*¹⁹) did not result in significant differences in WVP compared to the untreated film. In contrast, Fathi *et al.*¹⁶ found that UV-C radiation at 32 J cm^{-2} applied to either the film-forming solution or preformed film significantly decreased the WVP of the sesame protein isolate film. The slightly higher WVP for the FA + PFUV12 film is consistent with the microstructural features seen in the SEM images (Fig. 10). The presence of small pinholes and surface irregularities provides easier pathways for moisture sorption and diffusion, which likely counteract the barrier enhancement expected from cross-linking.

3.6 Film solubility

The addition of FA to soy protein films had no significant effect on water solubility ($p > 0.05$), as shown in Fig. 8. The film solubility of SPI and FA + SPI films was found to be around 40%. The insignificant effect of FA addition on solubility aligns with the findings of Arabestani *et al.*⁵⁴ for bitter vetch (*Vicia ervilia*) protein-based films. In contrast, Insaward *et al.*³³ observed a decrease in film solubility with the addition of FA to the SPI film. However, FA + UV-C treatment of preformed films gradually decreased film solubility as the radiation dose increased, and the FA + PFUV12 film demonstrated the lowest solubility at 37.49%. Conversely, FA + UV-C treatment of the film-forming solution resulted in a slight, insignificant increase in film solubility compared to the control. Overall, the film solubility of all samples in our study was not statistically different from that of the control. This insignificant difference in film solubility may also be attributed to the highly hydrophilic nature of the SPI film. Our findings align with those of Díaz *et al.*¹⁸ who investigated whey protein films. In contrast, Fathi *et al.*¹⁶ observed a significant reduction in film solubility in sesame protein isolate films after exposure to UV-C at 32.6 J m^{-2} . In addition, the authors noted that UV-C treatments, whether applied to the film-forming solution or to the preformed film, yielded similar results.

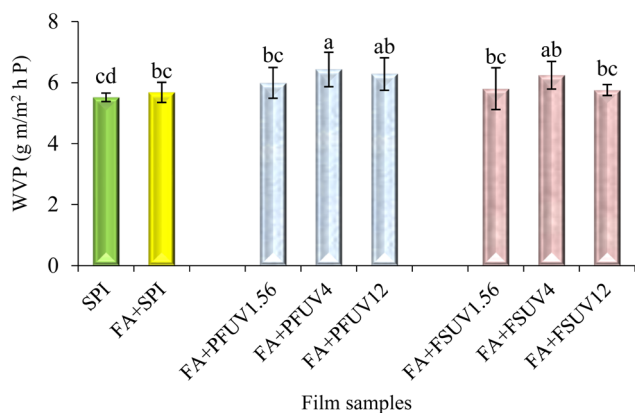


Fig. 7 WVP of treated and untreated soy protein isolate films.

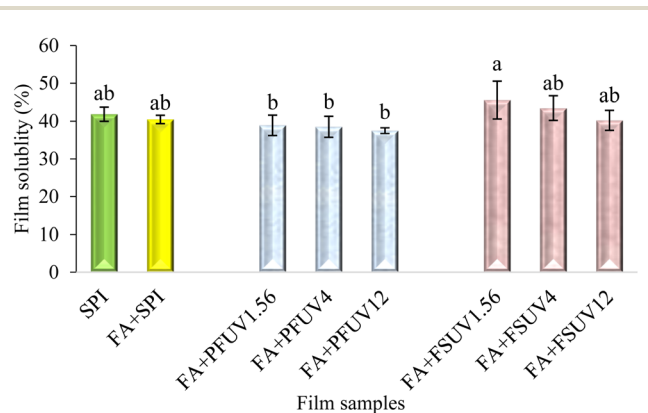


Fig. 8 Film solubility of treated and untreated soy protein isolate films.



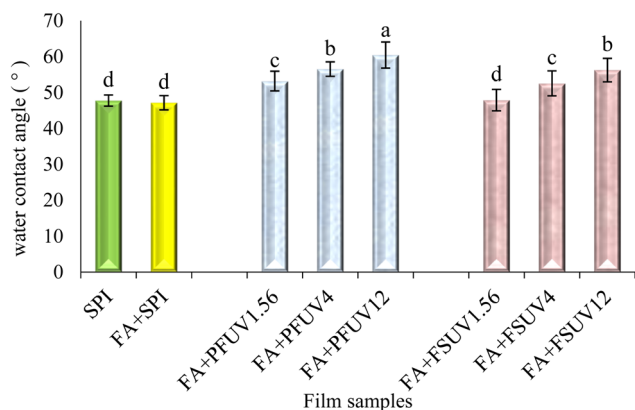


Fig. 9 Film hydrophobicity of treated and untreated soy protein isolate films.

3.7 Film hydrophobicity

The WCA of a water droplet with a film surface indicates the surface hydrophobicity. The hydrophobicity of treated and untreated SPI films is illustrated in Fig. 9. The SPI and FA + SPI films showed similar contact angles, around 50°. This suggests that the film samples had a hydrophilic surface, a characteristic of most protein films. The contact angles of FA + UV-C-treated films ranged from 47° to 60°. The contact angle of the FA + UV-C film exposed to 1.56 J cm⁻² was significantly greater ($p \leq 0.05$) than that of the control film. A significant increase in contact angle was observed with increasing UV-C dose, with the FA + PFUV12 film possessing the greatest contact angle of 60.40°. Nonetheless, the surface remained hydrophilic, as the WCA was below 90°.

However, FA + UV-C treatment of film-forming solutions had less effect on the film surface's hydrophobicity compared to preformed films. The WAC of the films also increased with higher UV-C doses, but to a lesser extent than with the preformed film treatment. According to Fathi *et al.*¹⁶ increased protein film surface hydrophobicity following UV-C irradiation is possible due to the development of cross-linking and the reduction of unbound hydrophilic groups within the polypeptide chains. In addition, Kristo *et al.*⁵⁵ also illustrated that this may be due to UV-induced conformational changes, which, in turn, result in the exposure of hydrophobic regions that, in

a native state, are buried inside the protein structure. The higher effectiveness of UV-C treatment of preformed films than the treatment of film-forming solutions may be attributed to the higher protein concentration in preformed (*i.e.*, dried) films. This higher concentration leads to the closer proximity of the polypeptide chains, thereby facilitating protein cross-linking at the surface. A similar result has also been reported by Fathi *et al.*¹⁶ for sesame protein isolate films.

3.8 Optical properties

Film transparency and color parameters are tabulated in Table 2. Transparency was expressed in % transmittance. Both the addition of ferulic acid and UV-C curing were found to impact film transparency significantly. The FA + SPI film exhibited a transmittance of 61.90%, which is statistically lower than that of the control (70.21%). The decline in transparency upon FA addition may be attributed to protein aggregation induced by ferulic acid-induced cross-linking and the formation of colored products from phenolic-protein reactions.^{56,57} This finding aligns with Insaward *et al.*³³ who reported similar results for soy protein films incorporating ferulic, caffeic, and gallic acids. However, this finding contrasts with that of Wang & Xiong,⁴⁸ who found that the addition of oxidized FA at 2.5% and 5.0% did not result in significant changes in the transparency of whey protein isolate films. Our study also observed that FA + UV-C treatment resulted in a decrease in film transparency as the UV-C dose increased. However, FA + UV-C treatment of both the preformed film and film-forming solution exhibited similar effects. The most significant effect was observed at higher UV-C doses (4.00 and 12.00 J cm⁻²), where the film samples exhibited a transmittance of approximately 50%. Cetinel *et al.*⁵⁸ noted that UV radiation can induce protein cross-linking through the recombination of aromatic amino acid-free radicals, particularly Tyr[•], and it has also been reported that radiation is among the major factors facilitating cataract formation or opacification of the ocular lens, which is caused by protein aggregation. The same mechanism may be responsible for the reduction in transparency of protein films upon exposure to UV-C. Schmid *et al.*⁵⁹ also reported a similar finding for whey protein isolate films.

The CIELAB color parameters of the film samples are summarised in Table 2. The addition of FA did not affect any parameters, particularly L^* , a^* , b^* , hue angle, and chroma, of

Table 2 Transparency and color parameters of untreated and treated SPI films^a

Film samples	L^*	a^* ^{ns}	b^*	Hue angle (°)	Chroma	%Transmittance
Control	90.44 ± 0.87 ^{ab}	-1.87 ± 0.13	17.91 ± 2.01 ^d	95.96 ± 0.54 ^{ab}	18.01 ± 2.10 ^d	70.21 ± 1.53 ^a
FA + SPI	90.01 ± 0.77 ^{bc}	-2.01 ± 0.16	18.65 ± 2.29 ^{cd}	96.15 ± 0.75 ^{ab}	18.76 ± 2.28 ^{cd}	61.90 ± 1.72 ^b
FA + PFUV1.56	90.79 ± 0.69 ^{ab}	-2.18 ± 0.24	19.53 ± 1.95 ^{cd}	96.38 ± 0.54 ^{ab}	19.66 ± 1.96 ^{cd}	56.83 ± 2.47 ^c
FA + PFUV4	91.13 ± 0.76 ^a	-1.87 ± 0.13	19.53 ± 2.29 ^{cd}	95.50 ± 0.34 ^b	19.62 ± 2.38 ^{cd}	54.91 ± 0.69 ^{cd}
FA + PFUV12	90.57 ± 1.06 ^{ab}	-1.66 ± 0.15	21.35 ± 2.70 ^{bc}	94.48 ± 0.39 ^d	21.42 ± 2.71 ^{bc}	51.73 ± 0.76 ^e
FA + FSUV1.56	90.49 ± 1.11 ^{ab}	-2.09 ± 0.24	19.44 ± 3.06 ^{cd}	96.18 ± 0.40 ^{ab}	19.56 ± 3.06 ^{cd}	62.73 ± 1.60 ^b
FA + FSUV4	90.12 ± 0.74 ^{bc}	-2.13 ± 0.27	22.45 ± 3.07 ^{ab}	95.42 ± 0.16 ^b	22.54 ± 3.09 ^{ab}	52.41 ± 1.33 ^{de}
FA + FSUV12	89.36 ± 1.25 ^c	-1.96 ± 0.20	24.89 ± 4.80 ^a	94.58 ± 0.49 ^c	24.97 ± 4.80 ^a	52.36 ± 0.85 ^{de}

^a Mean ± SD of three replicates. Sample means within a column that does not share a common superscript letter differ significantly at $p = 0.05$. ^{ns} Sample means within the column do not differ significantly at $p = 0.05$.



SPI films. The hue angle of the control and FA + SPI films was around 96° , which is close to the yellow hue angle (90°). However, adding phenolic compounds to protein films generally enhanced yellowness due to the colored product resulting from the reaction between phenolic compounds and proteins.⁶⁰ In another study, Insaward *et al.*³³ reported an increase in yellowness when ferulic, caffeic, or gallic acid was added to soy protein films. This discoloration got even more pronounced upon oxidation of the phenolic compound to its corresponding quinone. An increment in yellowness in the fish myofibrillar protein film treated with ferulic acid has also been documented by Prodpran *et al.*⁶¹ However, our study did not observe a significant increase in yellowness following the addition of FA.

At lower doses, FA + UV-C treatment of either preformed films or film-forming solutions did not have a significant effect on the color parameters of the films ($p > 0.05$). However, FA + UV-C treatment of preformed films at 12 J cm^{-2} and the treatment of film-forming solutions at 4 and 12 J cm^{-2} caused a significant change in $+b^*$. This, in turn, resulted in a shift of the hue angle towards a lower value and an increase in chroma, implying that the samples became more intense in yellowness as they appeared to the naked eye. In one study on whey protein films, Diaz *et al.*¹⁸ observed that UV exposure of the film-forming solution produced a more intense yellow color than that of the preformed film. This may be due to the fact that the greater molecular mobility in film-forming solutions facilitates photochemical reactions induced by UV.

UV treatment has also been reported to increase yellowing in whey protein films,³⁹ and in soy protein films without phenolic addition.^{19,24} However, Rhim & Gennadios²³ reported an opposing result, where UV-C was found to cause a reduction in the yellowness of zein films. The authors proposed that UV-C radiation may prompt the degradation of the pigment, contributing to the decrease in yellowness in zein protein. In another study, Micard *et al.*²¹ found no evidence of a significant effect of UV-C on the color of wheat gluten films. In our research, in addition to the direct impact of UV-C on the protein

film, we have predicted that UV-C may accelerate the oxidation of ferulic acid into the corresponding quinone, thereby increasing the chroma of the film samples.

3.9 Film microstructure

The cross-sectional structure of selected film samples is depicted in Fig. 10. The SPI, FA + SPI, FA + PFUV1.56, FA + PFUV12, FA + FSUV1.56, and FA + FSUV12 films were chosen for microstructure analysis. All the film samples appeared quite homogeneous in terms of their cross-sectional structure. The FA + UV-C films appeared to have a slightly more homogeneous microstructure than the control and FA + SPI films. In a study conducted by Zhang *et al.*,³⁶ it was found that incorporating 5% ferulic acid into the soy protein/chitosan composite film led to a more uniform, densely packed structure compared to the control film, which showed some inhomogeneous zones and small pores. Another study observed that ferulic acid at 50 mg/100 g in a bitter vetch (*Vicia ervilia*) protein film produced a film with more compactness and continuous zones, whereas the control sample presented discontinuous zones and some small pores.⁵⁴

In our study, compared to FA + UV treatment of the film-forming solution at 12 J cm^{-2} , the preformed film exposed to the same UV-C dose appeared to have more pinholes and microvoids in its structure. This may be because the preformed films are exposed to UV-C after drying, during which the polymer chains have limited mobility. This can cause uneven UV-induced cross-linking, potentially leading to localized shrinkage or micro-fractures. Such surface discontinuities are typically associated with higher hydrophilicity, and greater moisture transmission could indicate lower barrier properties. In contrast, solution-treated films form cross-links within a fluid matrix, resulting in a more consistent network with fewer pinholes. In one study, Fathi *et al.*¹⁶ found that UV-C exposure of a film-forming solution produced fewer irregularities and a more compact, denser sesame protein film. Conversely, UV-C treatment of preformed films resulted in films with more

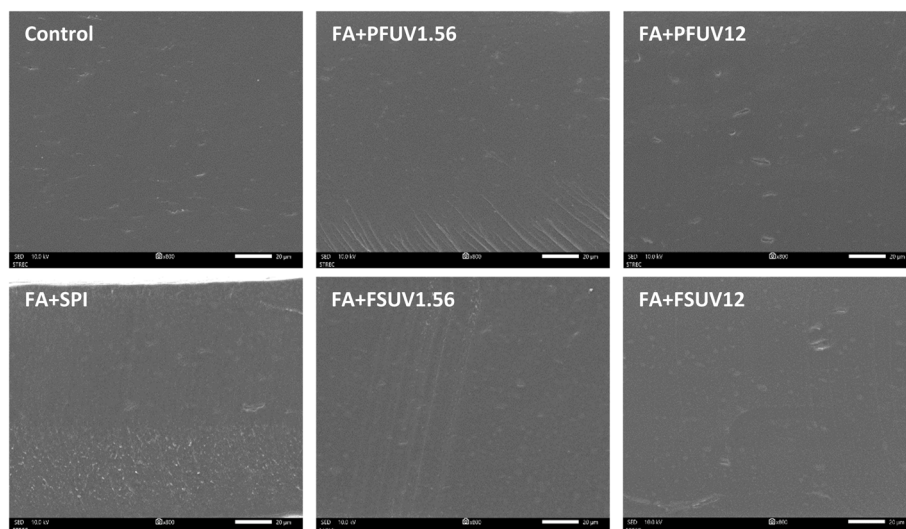


Fig. 10 Cross-sectional scanning electron micrographs of ferulic acid-added and/or UV-treated soy protein films obtained at $800\times$ magnification.



pinholes and minor cracks. These cracks are possibly due to internal brittleness and phase separation within the film matrix.

4 Conclusion

This study aimed to evaluate the effects of FA incorporation and FA + UV-C irradiation on the properties of SPI films. FA + UV-C irradiation at a higher dose (12.00 J cm^{-2}) significantly increased TS, EAB, film transparency, and WCA, and also led to a yellowish color, while moisture barrier properties, such as WVP and solubility, showed no significant improvement. The findings suggest that combining natural cross-linkers, such as FA, with UV-C at 12 J cm^{-2} treatment of the film-forming solution enhances mechanical strength, whereas applying the treatment to the pre-formed film improves the overall performance of biodegradable films, making it more suitable for simple industrial applications. This sustainable approach addresses the growing demand for environmentally friendly packaging that maintains product quality while minimizing its environmental impact. However, further optimization is still needed to adjust the concentration of FA or increase the UV-C dose for enhancement of the functional properties of the films and to improve key barrier attributes such as WVP, water solubility, and WAC. In addition, future research is needed to evaluate how these films perform during actual food storage. To sum up, the use of FA in conjunction with UV-C irradiation at higher doses significantly improved the mechanical properties of SPI films. This contributes to the development of more sustainable food packaging options that could, in some cases, substitute for conventional plastics and reduce environmental impact.

Author contributions

Md Shakil: investigation, formal analysis, data curation, and writing – original draft. Tanjina Akter: investigation, formal analysis, data curation, and writing – original draft. Nonhacha Thanathornvarakul: data curation, writing – original draft, and writing – review & editing. Thanachan Mahawanich: conceptualization, data curation, funding acquisition, project administration, supervision, writing – original draft, and writing – review & editing.

Conflicts of interest

The authors declare that they have no known competing financial interests or personal relationships that could have appeared to influence the work reported in this paper.

Data availability

The datasets generated and/or analyzed during this study are included in this manuscript.

Acknowledgements

This research is supported in part by the scholarship program for ASEAN or Non-ASEAN Countries of the Chulalongkorn University.

References

- 1 X. Pei, H. Jiao, H. Fu, X. Yin and L. Zhang, Facile construction of a highly dispersed Pt nanocatalyst anchored on biomass-derived N/O-doped carbon nanofibrous microspheres and its catalytic hydrogenation, *ACS Appl. Mater. Interfaces*, 2020, **12**, 51459–51467.
- 2 A. Nestic, S. Meseldzija, G. Cabrera-Barjas and A. Onjia, Novel biocomposite films based on high methoxyl pectin reinforced with zeolite Y for food packaging applications, *Foods*, 2022, **11**, 360.
- 3 Z. Qi, B. Wang, C. Sun, M. Yang, X. Chen, D. Zheng and Y. Zhang, Comparison of properties of poly (lactic acid) composites prepared from different components of corn straw fiber, *Int. J. Mol. Sci.*, 2022, **23**, 6746.
- 4 W. Qu, T. Guo, X. Zhang, Y. Jin, B. Wang and H. Wahia, Preparation of tuna skin collagen–chitosan composite film improved by sweep frequency pulsed ultrasound technology, *Ultrason. Sonochem.*, 2022, **82**, 105876.
- 5 C. L. Reichert, E. Bugnicourt, M. B. Coltelli, P. Cinelli, A. Lazzeri, I. Canesi, *et al.*, Bio-based packaging: materials, modifications, industrial applications and sustainability, *Polymers*, 2020, **12**, 1558.
- 6 S. Nanda, B. R. Patra, R. Patel, J. Bakos and A. K. Dalai, Innovations in applications and prospects of bioplastics and biopolymers: a review, *Environ. Chem. Lett.*, 2022, **20**, 379–395.
- 7 R. A. Rosenbloom and Y. Zhao, Hydroxypropyl methylcellulose or soy protein isolate-based edible, water-soluble, and antioxidant films for safflower oil packaging, *J. Food Sci.*, 2021, **86**, 129–139.
- 8 J. Wu, Q. Sun, H. Huang, Y. Duan, G. Xiao and T. Le, Enhanced physico-mechanical, barrier and antifungal properties of soy protein isolate film by incorporating both plant-sourced cinnamaldehyde and facile synthesized zinc oxide nanosheets, *Colloids Surf., B*, 2019, **180**, 31–38.
- 9 Z. A. Maryam Adilah, B. Jamilah and Z. A. Nur Hanani, Functional and antioxidant properties of protein-based films incorporated with mango kernel extract for active packaging, *Food Hydrocolloids*, 2018, **74**, 207–218.
- 10 J. Duan, Q. Zhou, M. Fu, M. Cao, M. Jiang and X. Duan, Research on properties of edible films prepared from Zein, soy protein isolate, wheat gluten protein by adding beeswax, *Food Bioprocess Technol.*, 2023, **16**, 2443–2454.
- 11 A. V and L. S. Badwaik, Recent advancement in improvement of properties of polysaccharides and proteins based packaging film with added nanoparticles: A review, *Int. J. Biol. Macromol.*, 2022, **203**, 515–525.
- 12 D. Shukla, N. K. Nandi, B. Singh, A. Singh, B. Kumar, R. K. Narang and C. Singh, Ferulic acid-loaded drug



- delivery systems for biomedical applications, *J. Drug Delivery Sci. Technol.*, 2022, 75, 103621.
- 13 G. Strauss and S. M. Gibson, Plant phenolics as cross-linkers of gelatin gels and gelatin-based coacervates for use as food ingredients, *Food Hydrocolloids*, 2004, 18, 81–89.
 - 14 N. Cao, Y. Fu and J. He, Preparation and physical properties of soy protein isolate and gelatin composite films, *Food Hydrocolloids*, 2007, 21, 1153–1162.
 - 15 M. Correia, M. T. Neves-Petersen, P. B. Jeppesen, S. Gregersen and S. B. Petersen, UV-Light Exposure of Insulin: Pharmaceutical Implications upon Covalent Insulin Dityrosine Dimerization and Disulphide Bond Photolysis, *PLoS One*, 2012, 7, e50733.
 - 16 N. Fathi, H. Almasi and M. K. Pirouzifard, Effect of ultraviolet radiation on morphological and physicochemical properties of sesame protein isolate based edible films, *Food Hydrocolloids*, 2018, 85, 136–143.
 - 17 N. Sherstneva, K. Ryazantseva, E. Agarkova and D. Myalenko, Investigation of the film-forming ability of proteins subjected to UV treatment for the dairy industry development, *IOP Conf. Ser. Earth Environ. Sci.*, 2022, 1112, 012080.
 - 18 O. Diaz, D. Candia and Á. Cobos, Effects of ultraviolet radiation on properties of films from whey protein concentrate treated before or after film formation, *Food Hydrocolloids*, 2016, 55, 189–199.
 - 19 A. Gennadios, J. W. Rhim, A. Handa, C. L. Weller and M. A. Hanna, Ultraviolet Radiation Affects Physical and Molecular Properties of Soy Protein Films, *J. Food Sci.*, 1998, 63, 225–228.
 - 20 C.-C. Liu, A. M. Tellez-Garay and M. E. Castell-Perez, Physical and mechanical properties of peanut protein films, *LWT-Food Sci. Technol.*, 2004, 37, 731–738.
 - 21 V. Micard, R. Belamri, M. Morel and S. Guilbert, Properties of chemically and physically treated wheat gluten films, *J. Agric. Food Chem.*, 2000, 48, 2948–2953.
 - 22 C. G. Otoni, R. J. Avena-Bustillos, B.-S. Chiou, C. Bilbao-Sainz, P. J. Bechtel and T. H. McHugh, Ultraviolet-B radiation induced cross-linking improves physical properties of cold- and warm-water fish gelatin gels and films, *J. Food Sci.*, 2012, 77, E215–E223.
 - 23 J. W. Rhim, A. Gennadios, D. Fu, C. L. Weller and M. A. Hanna, Properties of Ultraviolet Irradiated Protein Films, *LWT-Food Sci. Technol.*, 1999, 32, 129–133.
 - 24 J. W. Rhim, A. Gennadios, A. Handa, C. L. Weller and M. A. Hanna, Solubility, Tensile, and Color Properties of Modified Soy Protein Isolate Films, *J. Agric. Food Chem.*, 2000, 48, 4937–4941.
 - 25 A. Gennadios, J. W. Rhim, A. Handa, C. L. Weller and M. A. Hanna, MS 97- Ultraviolet Radiation Affects Physical and 2347 Molecular Properties of Soy Protein Films, *J. Food Sci.*, 1998, 63, 225–228.
 - 26 M. Puchala and H. Schuessler, Oxygen effect in the radiolysis of proteins: IV. Myoglobin, *Int. J. Pept. Protein Res.*, 1995, 46, 326–332.
 - 27 M. Ressouany, C. Vachon and M. Lacroix, Irradiation dose and calcium effect on the mechanical properties of cross-linked caseinate films, *J. Agric. Food Chem.*, 1998, 46, 1618–1623.
 - 28 Y. Cho, J. S. Yang and K. Bin Song, Effect of ascorbic acid and protein concentration on the molecular weight profile of bovine serum albumin and β -lactoglobulin by γ -irradiation, *Food Res. Int.*, 1999, 32, 515–519.
 - 29 A. Insaward, K. Duangmal and T. Mahawanich, Mechanical, Optical, and Barrier Properties of Soy Protein Film As Affected by Phenolic Acid Addition, *J. Agric. Food Chem.*, 2015, 63, 9421–9426.
 - 30 Y. K. Al-Hilaly, L. Biasetti, B. J. F. Blakeman, S. J. Pollack, S. Zibae, A. Abdul-Sada, J. R. Thorpe, W.-F. Xue and L. C. Serpell, The involvement of dityrosine crosslinking in α -synuclein assembly and deposition in Lewy Bodies in Parkinson's disease, *Sci. Rep.*, 2016, 6, 39171.
 - 31 The Definitive Guide to ASTM D882 Tensile Testing of Thin Plastic Film, <https://www.instron.com/en/testing-solutions/astm-standards/astm-d882>, (accessed 14 October 2024).
 - 32 ASTM E96 - 95 Standard Test Methods for Water Vapor Transmission of Materials | Building CodeHub, <https://codehub.building.govt.nz/resources/astm-e96-95>, (accessed 15 October 2024).
 - 33 A. Insaward, K. Duangmal and T. Mahawanich, Mechanical, Optical, and Barrier Properties of Soy Protein Film As Affected by Phenolic Acid Addition, *J. Agric. Food Chem.*, 2015, 63, 9421–9426.
 - 34 W. M. Ikhmal, M. Y. N. Yasmin, M. F. M. Fazira, W. A. W. Rafizah, W. B. Wan Nik and M. G. M. Sabri, Anticorrosion Coating using Olea sp. Leaves Extract, *IOP Conf. Ser. Mater. Sci. Eng.*, 2018, 344, 012028.
 - 35 Z. A. Maryam Adilah, F. Han Lyn, B. Nabilah, B. Jamilah, C. Gun Hean and Z. A. Nur Hanani, Enhancing the physicochemical and functional properties of gelatin/graphene oxide/cinnamon bark oil nanocomposite packaging films using ferulic acid, *Food Packag. Shelf Life*, 2022, 34, 100960.
 - 36 C. Zhang, X. F. Guo, Y. Ma and X. Y. Zhao, Ferulic Acid and its Oxide Enhance Performance of Soy Protein-Isolate/Chitosan Composite Films, *Appl. Mech. Mater.*, 2015, 716–717, 28–31.
 - 37 A. Sionkowska, J. Skopinska, M. Wisniewski, A. Leznicki and J. Fisz, Spectroscopic studies into the influence of UV radiation on elastin hydrolysates in water solution, *J. Photochem. Photobiol., B*, 2006, 85, 79–84.
 - 38 D. A. Malencik and S. R. Anderson, Dityrosine as a product of oxidative stress and fluorescent probe, *Amino Acids*, 2003, 25, 233–247.
 - 39 H. Terryn, J.-P. Vanhelleputte, A. Maquille and B. Tilquin, Chemical analysis of solid-state irradiated human insulin, *Pharm. Res.*, 2006, 23, 2141–2148.
 - 40 D. Balasubramanian and R. Kanwar, in *Oxygen/Nitrogen Radicals: Cell Injury and Disease*, Springer, 2002, pp. 27–38.
 - 41 P. Nuthong, S. Benjakul and T. Prodpran, Effect of phenolic compounds on the properties of porcine plasma protein-based film, *Food Hydrocolloids*, 2009, 23, 736–741.



- 42 S. Ou, Y. Wang, S. Tang, C. Huang and M. G. Jackson, Role of ferulic acid in preparing edible films from soy protein isolate, *J. Food Eng.*, 2005, **70**, 205–210.
- 43 I. Arcan and A. Yemenicioğlu, Incorporating phenolic compounds opens a new perspective to use zein films as flexible bioactive packaging materials, *Food Res. Int.*, 2011, **44**, 550–556.
- 44 B. C. Smith, *Fundamentals of Fourier Transform Infrared Spectroscopy*, CRC Press, Boca Raton, 2nd edn, 2011.
- 45 T. G. Mayerhöfer and J. Popp, Understanding the Role of the Evanescent Field in Attenuated Total Reflection (ATR) Spectroscopy, *Appl. Spectrosc.*, 2025, 00037028251358400.
- 46 T. Akter, M. Shakil and T. Mahawanich, UV-C induced modification of heat-cured soy protein films: Mechanical, optical, barrier, and morphological properties, *Future Foods*, 2025, **11**, 100663.
- 47 Z. Ren, Y. Ning, J. Xu, X. Cheng and L. Wang, Eco-friendly fabricating Tara pod extract-soy protein isolate film with antioxidant and heat-sealing properties for packaging beef tallow, *Food Hydrocolloids*, 2024, **153**, 110041.
- 48 Y. Wang and Y. L. Xiong, Physicochemical and Microstructural Characterization of Whey Protein Films Formed with Oxidized Ferulic/Tannic Acids, *Foods*, 2021, **10**, 1599.
- 49 E. M. Masutani, C. K. Kinoshita, T. T. Tanaka, A. K. D. Ellison and B. A. Yoza, Increasing Thermal Stability of Gelatin by UV-Induced Cross-Linking with Glucose, *Int. J. Biomater.*, 2014, **2014**, 979636.
- 50 M. Schmid, T. K. Prinz, K. Müller and A. Haas, UV Radiation Induced Cross-Linking of Whey Protein Isolate-Based Films, *Int. J. Polym. Sci.*, 2017, **2017**, 1846031.
- 51 A. González, M. C. Strumia and C. I. Alvarez Igarzabal, Cross-linked soy protein as material for biodegradable films: Synthesis, characterization and biodegradation, *J. Food Eng.*, 2011, **106**, 331–338.
- 52 J. Wang, W. Burton Navicha, X. Na, W. Ma, X. Xu, C. Wu and M. Du, Preheat-induced soy protein particles with tunable heat stability, *Food Chem.*, 2021, **336**, 127624.
- 53 O. Díaz, D. Candia and Á. Cobos, Whey protein film properties as affected by ultraviolet treatment under alkaline conditions, *Int. Dairy J.*, 2017, **73**, 84–91.
- 54 A. Arabestani, M. Kadivar, M. Shahedi, S. A. H. Goli and R. Porta, The effect of oxidized ferulic acid on physicochemical properties of bitter vetch (*Vicia ervilia*) protein-based films, *J. Appl. Polym. Sci.*, 2016, **133**(2), DOI: [10.1002/app.42894](https://doi.org/10.1002/app.42894).
- 55 E. Kristo, A. Hazizaj and M. Corredig, Structural Changes Imposed on Whey Proteins by UV Irradiation in a Continuous UV Light Reactor, *J. Agric. Food Chem.*, 2012, **60**, 6204–6209.
- 56 C.-H. Tang, Y. Jiang, Q.-B. Wen and X.-Q. Yang, Effect of transglutaminase treatment on the properties of cast films of soy protein isolates, *J. Biotechnol.*, 2005, **120**, 296–307.
- 57 J. B. Yi, Y. T. Kim, H. J. Bae, W. S. Whiteside and H. J. Park, Influence of Transglutaminase-Induced Cross-Linking on Properties of Fish Gelatin Films, *J. Food Sci.*, 2006, **71**, E376–E383.
- 58 S. Cetinel, V. Semenchenko, J.-Y. Cho, M. G. Sharaf, K. F. Damji, L. D. Unsworth and C. Montemagno, UV-B induced fibrillization of crystallin protein mixtures, *PLoS One*, 2017, **12**, e0177991.
- 59 M. Schmid, J. Held, F. Hammann, D. Schlemmer and K. Noller, Effect of UV-Radiation on the Packaging-Related Properties of Whey Protein Isolate Based Films and Coatings, *Packag. Technol. Sci.*, 2015, **28**, 883–899.
- 60 H. M. Rawel, D. Czajka, S. Rohn and J. Kroll, Interactions of different phenolic acids and flavonoids with soy proteins, *Int. J. Biol. Macromol.*, 2002, **30**, 137–150.
- 61 T. Prodpran, S. Benjakul and S. Phatcharat, Effect of phenolic compounds on protein cross-linking and properties of film from fish myofibrillar protein, *Int. J. Biol. Macromol.*, 2012, **51**, 774–782.

